Travelling with a parasite: the evolution of resistance and dispersal syndromes during experimental range expansion

Giacomo Zilio[1#*], Louise S. Nørgaard[2#], Claire Gougat-Barbera[1], Matthew D. Hall[2], Emanuel A. Fronhofer[1] & Oliver Kaltz[1*]

Giacomo Zilio[1#*], gcm.zilio@gmail.com, ORCID ID: https://orcid.org/0000-0002-4448-3118

Louise S. Nørgaard[2#], lnorga10@hotmail.com, ORCID ID: https://orcid.org/0000-0002-0938-0017

Claire Gougat-Barbera[1], claire.gougat-barbera@umontpellier.fr, ORCID ID: unavailable

Matthew D. Hall[2], matthew.hall@monash.edu, ORCID ID: 0000-0002-4738-203X

Emanuel A. Fronhofer[1], emanuel.fronhofer@umontpellier.fr, ORCID ID: https://orcid.org/0000-0002-2219-784X

Oliver Kaltz[1*], oliver.kaltz@umontpellier.fr, ORCID ID: https://orcid.org/0000-0002-7154-0456

[1] ISEM, University of Montpellier, CNRS, EPHE, IRD, Montpellier, France.

[2] School of Biological Sciences and Centre for Geometric Biology, Monash University, Melbourne, Australia

[#] Shared first-author contribution

* Corresponding author: gcm.zilio@gmail.com, oliver.kaltz@umontpellier.fr

Abstract

Rapid evolutionary change during range expansions can lead to diverging range core and front populations, with the emergence of dispersal syndromes (coupled responses in dispersal and life-history traits). Besides intraspecific effects, range expansions may be impacted by interspecific interactions such as parasitism. Yet, despite the potentially large impact of parasites imposing additional selective pressures on the host, their role on range expansions remains largely unexplored. Using microcosm populations of the ciliate *Paramecium caudatum* and its bacterial parasite *Holospora undulata*, we studied experimental range expansions under parasite presence or absence. We found that the interaction of range expansion and parasite treatments affected the evolution of host dispersal syndromes. Namely, front populations showed different associations of population growth parameters and swimming behaviours than core populations, indicating divergent evolution. Parasitism reshaped trait associations, with hosts evolved in the presence of the parasite exhibiting overall increased resistance and reduced dispersal. Nonetheless, when comparing infected range core and front populations, we found a positive association, suggesting joint evolution of resistance and dispersal at the front. We conclude that host-parasite interactions during range expansions can change evolutionary trajectories; this in turn may feed back on the ecological dynamics of the range expansion and parasite epidemics.

Keywords

Dispersal syndromes, eco-evolutionary dynamics, host-parasite interactions, invasion front, range expansion, resistance

Introduction

Species range expansions are increasing in frequency in response to rapidly changing environments [1] and becoming crucial to reducing the risk of extinction [2]. While ecological and evolutionary processes have been well explored for single species, we are still lacking a good community perspective of range shifts [3,4]. Species might rarely "travel alone", and it is conceivable that interactions with other organisms facilitate or slow down spatial spread, and add new selection pressures while a species is spreading.

Antagonistic species interactions have been suggested to be a major factor defining species ranges [5,6]. Parasitism, for example, are ubiquitous and exert strong demographic and evolutionary pressures on the host [7,8], which can limit geographic ranges as has been shown in some theoretical models [9–11]. Parasites may re-enforce range limits by reducing dispersal and/or by imposing additional mortality in already small populations at the range front. Such modifications of the ecological dynamics seems to limit the spread of the invasive cane toad (*Rhinella marina*) in Australia [12,13], and also play a role in other natural systems [14–16]. The evolution of counter-adaptation against parasites may remove such range limits, but also lead to more complex outcomes if parasite-mediated selection affects the evolution of other life-history traits known to be selected at range fronts. Novel trait combinations may then produce eco-evolutionary feedbacks influencing rates of spatial spread of both the host species and the parasite. This may cause knock-on effects on interactions with other species in the community [17,18] or increase the risk of spill-over of disease [19,20]. Thus, understanding how parasites shape evolutionary trajectories of phenotypic traits in a range expansion context is also of major interest to conservation, disease control [21–23] or invasive species management [24].

Range expansions often involve stochastic genetic change in small vanguard front populations (via drift or founder bias), but also the concerted evolution of dispersal, life-history, behaviour or physiology, often referred to as “dispersal syndrome” [25,26]. Typically range front populations may be populated by individuals with a coloniser phenotype, characterised, e.g., by high dispersal propensity and high reproductive rate. Kin selection and spatial assortative mating are then expected to reinforce such trait associations while the range front is expanding [27,28]. There is empirical and experimental evidence that such spatial selection is indeed a strong evolutionary force. Dispersal is a heritable trait in various biological systems and covariation with other traits has a genetic basis [29], making it possible for selection to drive multi-trait divergence between core and front populations [30,31]. An example is the above-mentioned cane toad, where the evolution of dispersal and other life-history traits promoted the speed of spread at the invasion front [32–34]. Similar results were found for the invasive ladybird *Harmonia axyridis* [35], and in laboratory range expansions using experimental evolution approaches [36–38].

81 We currently know relatively little about parasite-mediated selection at range fronts and its consequences
82 for dispersal syndrome evolution [3,4]. While a considerable bulk of literature exists on resistance evolution
83 in host-parasite metapopulations [39,40], there is no specific theory in the context of range expansion.
84 Intuitively, we may expect that virulent parasites select for increased resistance and that this removes a
85 parasite-imposed range speed limit. Such a case of resistance evolution has been found for populations of
86 the cane toad infested by lung-worms at the range margin [41,42]. Theory further suggests that natural
87 enemies select for changes in host dispersal. For example, parasite-induced fluctuations in host population
88 dynamics can modify environmental predictability and fitness expectations, and consequently favour
89 increased host dispersal [43,44]. Parasites may also select for plastic responses in dispersal, with sometimes
90 counter-intuitive consequences for the spread of infection [45].

91 However, few if any studies have considered the joint action of parasite-mediated selection and spatial
92 selection, and hence the interplay between the evolution of resistance and dispersal-related traits. Indeed,
93 selection for resistance can be rapid and strong, but also modify genetic correlations with other life-history
94 traits [46,47], often involving trade-offs [48,49] that constrain evolutionary trajectories. Hence, if selection
95 for resistance is uncorrelated with dispersal syndrome traits (or even positively correlated), counter-
96 adaptation against the natural enemy may simply remove the brake from range expansion. However, if
97 resistance trades off with expansion-relevant traits, such as dispersal or growth, the additional parasite-
98 mediated selection may shift populations to novel positions in multi-trait space, which finally may or may not
99 impede spatial spread.

100 Using experimental evolution, we investigated the effect of a parasite on the emergence of dispersal
101 syndromes. In a long-term experiment, we mimicked range expansions in interconnected microcosms of the
102 freshwater protist *Paramecium caudatum* and its bacterial parasite *Holospora undulata*. In a range front
103 treatment, the paramecia were constantly selected to disperse into a new microcosm, whereas in the range
104 core treatment, only the non-dispersing fraction of the population was maintained. Range and core
105 treatments were established for infected and uninfected populations. Evolved hosts were assayed for six
106 traits, including dispersal, resistance, population growth characteristics and swimming behaviour. We found
107 substantial divergence in multiple phenotypes in the trait space, attributable to the combined effect of our
108 experimental treatments. A dispersal syndrome emerged, with higher population equilibrium density and
109 movement tortuosity in the front treatment, and higher population growth rate and swimming speed in the
110 core treatment. Evolution with the parasite affected some of these trait relationships and additionally left
111 signatures in the observed levels of resistance and dispersal. Populations evolving with the parasite were
112 more resistant, in particular those in the range front treatment. In contrast, *Paramecium* originating from
113 parasitised populations generally dispersed less than their parasite-free counterparts. The parasite-driven
114 evolution of such novel multi-trait associations may influence the speed of range expansions, but also the

risk of spreading epidemics, which can have important implications for biological control or conservation management.

Material and methods

Study system

Paramecium caudatum is a freshwater filter-feeding ciliate with a world-wide distribution [50]. Ciliates typically exhibit a nuclear dimorphism: The "germ-line" micronucleus is active during the sexual stage, while the highly polyploid "somatic" macronucleus regulates gene expression during the asexual stage, when replication occurs through mitotic division. In this experiment, clonal populations were maintained asexually (max. 1-2 population doublings per day at constant 23°C) in 50 mL tubes, using a sterilised lettuce medium (1g dry weight of organic lettuce per 1.5l of Volvic™ mineral water), supplemented *ad libitum* with the bacterium *Serratia marcescens* as a food resource (referred to as "bacterised medium" or "medium", hereafter). The gram-negative bacterium *Holospora undulata* is an obligate parasite, infecting the micronucleus of *P. caudatum* [51]. The infection life cycle comprises both horizontal and vertical transmission. *Paramecium* ingest infectious forms from the aquatic environment, which subsequently colonise the micronucleus and differentiate into multiplying reproductive forms; these reproductive forms are vertically transmitted to the daughter cells of mitotically dividing hosts. The infection life cycle is completed when reproductive forms differentiate into infectious forms (c. 7 days post infection), which are then released during host cell division or upon host death. With accumulating parasite loads, infection reduces cell division and survival of the *Paramecium*, as well as dispersal [52–54]. Experimental evolution of resistance to this parasite was demonstrated in previous long-term experiments and can come at reproductive costs [55,56].

Experimental protocols

(i) Long-term range expansion experiment

<u>*Dispersal in two-patch systems*</u>

We used two-patch systems for this selection experiment (Supplementary Information, Fig. S1). The systems were built from two 14 mL plastic tubes ("core patch" and "front patch") interconnected by 5-cm silicon tubing (0.6 mm inner diameter) serving as a corridor through which the *Paramecium* can actively swim. We define dispersal as the active displacement of *P. caudatum* from the core patch to the front patch. In the long-term experiment, short episodes of dispersal (3h) alternated with periods of population growth and maintenance (1 week). For a dispersal episode, we filled the two-patch system with 9.5 mL of fresh bacterised medium and then blocked the corridor with a clamp. The core patch was filled with c. 8ml of culture containing *Paramecium* (≈ 2000 individuals), whereas the front patch was only topped up with non-

147 bacterised medium and was thus "empty". After removal of the clamp, *Paramecium* could freely disperse to
148 the front patch or to stay in the core. After three hours, we blocked the corridor and estimated the cell
149 density in the core and front patch, by sampling up to 1mL from each tube and counting the number of
150 individuals under a dissecting microscope. The dispersal rate is thus the number of dispersers divided by the
151 total number of individuals in the two-patch systems, divided by 3 hours.

152 *Range expansion treatments*

153 Two "range expansion" treatments were imposed. In the range front treatment, only *Paramecium* that
154 dispersed into the front patch were maintained and allowed to grow for 1 week until the next episode of
155 dispersal. Conversely, in the range core treatment, only the non-dispersing *Paramecium* were maintained
156 and allowed to regrow. These contrasting selection protocols were continued for a total of 26 cycles. The
157 front selection treatment mimics the leading front of range expansion or a biological invasion, with
158 populations continuously dispersing into a new microcosm. Populations from the range core treatment stay
159 in place and continuously lose emigrants. Each new growth cycle was started by placing on average 200
160 paramecia from front and core treatments in 20 mL of fresh bacterised medium, and equilibrium density was
161 then reached within the following 3-4 days. The experiment was conducted with a single host line [53]. This
162 line (63D) had undergone three years of parasite-free core selection prior to the present experiment; initially
163 started from a mix of strains, it has become fixed for a single cytochrome oxydase I haplotype [57].

164 *Parasite treatment*

165 Range core and front treatments were established for both infected and uninfected populations. The
166 parasites were taken from an experiment [53] that had already been imposing core and front selection on
167 infected 63D populations for about 8 months (30 cycles). Using standard protocols (see S2), we extracted
168 infectious forms of the parasite from 5 core selection lines and from 5 front selection lines, which were then
169 used to inoculate our new, naive 63D hosts. In other words, we continued range core and front treatments
170 for the parasite, but replaced the previous hosts by new unselected hosts. In addition to these 10 infected
171 selection lines, we established 3 uninfected front-selection lines and 3 uninfected core-selection lines as
172 controls, giving a total of 16 selection lines. After this initial inoculation of the experimental lines, we did not
173 interfere with epidemiological dynamics and all transmission occurred naturally over the course of the 26
174 new cycles of the long-term experiment. We routinely measured dispersal and population density (Fig. S4)
175 and verified the presence of infection in the parasite treatment.

176 **(ii) Phenotypic trait assays**

177 At the end of the long-term experiment, phenotypic trait assays for *Paramecium* from all 16 selection lines
178 were performed under common-garden conditions. Using a micropipette, we arbitrarily picked 4 uninfected
179 paramecia from each selection line and placed them individually in single 1.5 mL Eppendorf tubes filled with

180 bacterised medium, where they were allowed to grow for 2 weeks until small monoclonal lines had
181 established (c. 7-8 asexual generations). Each monoclonal line was then split into three technical replicates
182 and grown for a second common-garden period of 10 days in 50-mL tubes to obtain mass cultures for the
183 phenotype assays (16 selection lines x 4 monoclonal lines x 3 technical replicates = 64 monoclonal lines and
184 192 replicates, Fig. S3). Of the 64 monoclonal lines, one monoclonal line from the core treatment with
185 parasite did not grow and was lost, leaving us with 63 lines available to measure 6 phenotypic traits, as
186 follows.

187 *Resistance*

188 To measure resistance, the *Paramecium* were confronted with parasites from range core and front
189 treatments. To this end, we prepared inocula by extracting infectious forms from mixes of the 5 infected core
190 and the 5 infected front selection lines (for details of the protocol, see S2). For inoculation, c. 5000 paramecia
191 were placed in a volume of 25 mL in a 50-mL tube, to which we added 4.5 x 10^5 infectious forms (core-parasite
192 or front-parasite inoculum). In this way, we set up 4-8 inoculated tubes per host selection line, balanced
193 between the two parasite inocula (16 selection lines x 2-4 monoclonal lines x 2 technical replicates = 120
194 inoculated tubes). Four days post-inoculation, we fixed c. 20 individuals from each inoculated replicate with
195 lacto-aceto-orcein [51] and inspected them for absence or presence of infection using a phase-contrast
196 microscope (1000x magnification). We define resistance as the proportion of uninfected individuals in the
197 sample. Preliminary analysis showed that *Paramecium* from the four different selection treatments did not
198 differ in their resistance to the mixes of front or core parasites ($F_{3,12}$ = 0.44, n.s.); we therefore combined the
199 two inoculum sources into a single "infected" category for the main analysis. Note, however, that this does
200 not rule out the possibility of specific responses to range or core parasites in other host traits.

201 *Dispersal rate*

202 Dispersal was measured in linear 3-patch systems (50 mL tubes; Fig. S5), where uninfected *Paramecium*
203 dispersed from the middle tube into the two outer tubes (see SI for detailed protocol). This system
204 configuration allowed us to use bigger volumes of culture and thus obtain higher numbers of dispersers than
205 in 2-patch systems. Connections were opened for 3 h, dispersal rates were then estimated by counting the
206 *Paramecium* in samples from the central tube (500 µl) and from the combined two outer tubes (3 mL). We
207 employed technical replicates that had not been used for the resistance assay, and were kept in 30 mL of
208 fresh medium for several days prior to the dispersal test. One replicate per monoclonal line was tested (63
209 dispersal tests).

210 *Population growth rate and equilibrium density*

211 For the population growth assay, we placed groups of 5 arbitrarily picked *Paramecium* in 15-mL tubes filled
212 with 10 mL of bacterised medium. Over 9 days, we tracked densities in 24-h intervals, estimated from the

number of individuals present in 200-µL samples. We set up 6-12 tubes per host selection line (3 technical replicates per monoclonal line), with a total of 180 replicates. Only uninfected *Paramecium* were tested. For each tube, estimates of intrinsic population growth rate (r_0) were obtained by fitting a Beverton-Holt population growth model to each density time series, using a Bayesian approach [58],. For certain tubes we obtained unsatisfactory fits of equilibrium density; we therefore decided to use the mean density over the second half of the assay (day 5-9) as a proxy for equilibrium density ($\bar{N}$). A small fraction of 19 tubes (corresponding to 9 monoclonal lines from selection lines from range front and parasitism treatment) failed to grow and remained at very low density for unknown reasons; it was not possible to fit our population growth model to these data, and these replicates were therefore excluded from analysis.

Swimming speed and tortuosity

At the end of the above population growth assay, we assessed swimming behaviour, using an established pipeline of computer vision and automated video analysis to collect this data [59,60]. From a given tube, one sample of 119 µL was imaged under a Perfex Pro 10 stereomicroscope, using a Perfex SC38800 camera (15 frames per second; duration: 10 s; total magnification: 10x). Videos were analysed using the bemovi R-package [60], which provided individual-based data on swimming speed and the tortuosity of swimming trajectories (standard deviation of the turning angle distribution). Swimming speed and tortuosity were averaged over all individuals in a sample prior to analysis. A total of 63 samples (1 per monoclonal line) was used for analysis, giving 2-4 observations per host selection line. Three monoclonal lines (front parasite-exposed) went extinct prior to video recording.

Statistical analysis

All statistical analyses were performed with R v 4.2.0 [61], using Bayesian models with the “rstan” (version 2.21.5), “brms” (version 2.17.0) and “rethinking” (version 2.21) packages [62–64]. Focusing on the analysis of trait associations, we constructed a data matrix with the measurements of the 6 traits for 63 monoclonal lines (for resistance, the mean over the two technical replicates was calculated). To impute 24 missing observations (9 for $\bar{N}$ and r_0, 3 for swimming speed and tortuosity), we used the “mice” package version 3.14.0 [65] and took the mean of 1000 multiple imputations (24/378 imputed values). Trait distributions were standardized by using the standardize function of the “rethinking” package [64].

We then fitted five multivariate multilevel models, from the intercept to the full interaction model, using a normal error structure (chain length: warmup = 1,000 iterations, chain = 20,000 iterations). The explanatory factors of the full model were range expansion treatment (core vs front selection lines), parasite treatment (infected vs uninfected control selection lines) and their interaction, selection line identity was included as random term. Models were fitted with the default vaguely informative priors of the “brms” package. We compared and ranked the five models using the Watanabe–Akaike information criterion, WAIC [66], a

generalized version of the Akaike information criterion [67]. We used a conservative approach based on WAIC weights and not on the best ranked model. We averaged the posterior predictions of the models and calculated the relative importance (RI) of the explanatory variables. The RI corresponds to the sum of the respective WAIC model weights in which the explanatory variable was present. From this same data set and following the same procedure we also performed univariate analyses for each of the 6 traits. In addition, for a complementary graphical inspection of the results we used the above data matrix to carry out a principal component analysis (PCA).

Results

Multivariate analysis revealed signatures of selection history, with strong effects of range expansion treatment (relative importance, RI = 1.00) and parasitism treatment (RI = 0.77) on the observed phenotypic variation and covariation (Table 1). After model selection, the interaction between range expansion and parasitism (RI = 0.55) was retained in the best model fit (lowest WAIC; Model 5 in Table 1), indicating that the effect of spatial selection acted jointly with the presence of the parasite. In additional univariate analyses, all 6 traits showed signals of the two experimental treatments in combination or alone (Table 2, details for all traits in SI, Table S3-S8).

Table 1. Statistical models and parameters included in the main multivariate trait analysis and model averaging. Rows are the different models; the best model is highlighted in bold. Columns are the explanatory variables included with the corresponding WAIC, standard error of the WAIC and WAIC weights for each model. The RI row indicates the relative importance of the explanatory variables.

	Range expansion	Parasitism	Range * Parasitism	WAIC	SE	WAIC weight
Model 1				951.2	40.2	0.00
Model 2		X		952.3	39.5	0.00
Model 3	X			942.1	40.0	0.23
Model 4	X	X		942.2	39.5	0.22
Model 5	**X**	**X**	**X**	**940.4**	**39.1**	**0.55**
RI	1.00	0.77	0.55			

268 **Table 2**. Best model and WAIC weights from model averaging of single trait analysis. The explanatory
269 variables included in the best model are indicated with X. The complete list of the models for each trait is
270 given in the SI.
271

	Range expansion	Parasitism	Range * Parasitism	WAIC weight
Dispersal		X		0.28
Resistance	X	X	X	0.42
r_0	X	X	X	0.26
$\bar{N}$	X	X		0.23
Speed	X			0.62
Tortuosity	X			0.39

272

273 PCA visualizes the (co)variation in multivariate trait space (Fig. 1) and the relative contribution of the six
274 measured traits to the observed patterns of divergence among monoclonal lines (individual points in Fig. 1)
275 and combinations of treatments. As shown by the arrows in Fig. 1, the six traits have similar weight but
276 different orientation (Table S2; PCA loadings), with some pointing in opposite directions, indicative of trade-
277 offs. The details of the PCA are provided in Tables S1 and S2.

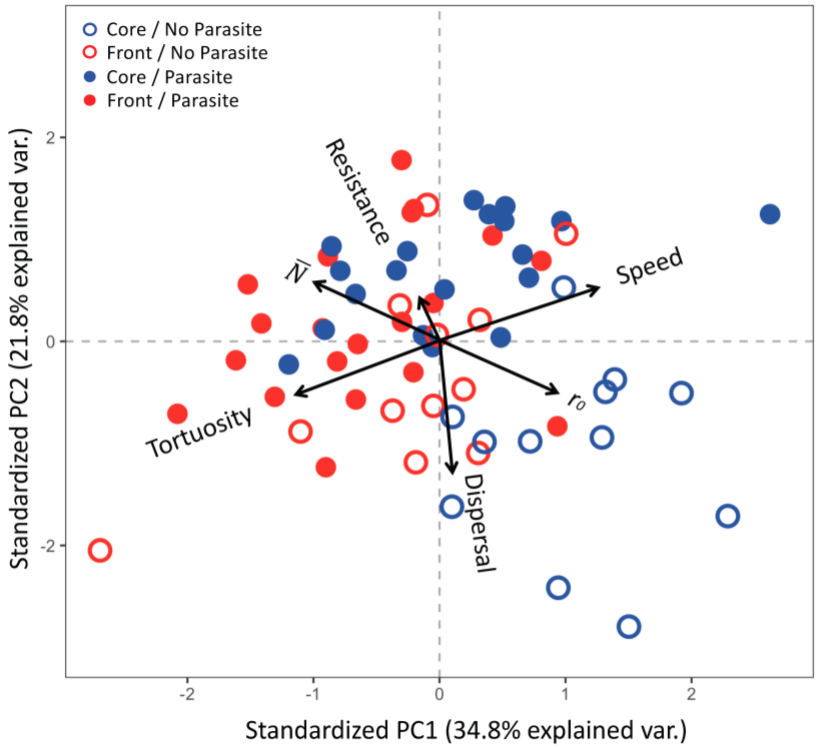

278

279 **Figure 1** PCA for six traits measured for *P. caudatum* from 4 long-term treatment combinations, showing the
280 first two principal component axes, PC1 and PC2. Each of the 63 points represents the average phenotypic
281 value of a given monoclonal line in multivariate space, with long-term treatment origins specified: range core
282 (blue) vs. range front (red) treatment; evolved in the presence (full circles) vs. absence (empty circles) of the
283 parasite *H. undulata*.

284 In long-term treatments without parasite, we observed a main pattern of divergence between range core
285 and front treatments along the horizontal PC1 axis (red vs blue open points Fig. 1). The direction and length
286 of the different arrows in Fig. 1 show that this was mainly driven by opposing trends in traits related to
287 demography and movement (r_0/ $\bar{N}$and speed / tortuosity have highest PC 1 loadings, Table S2). Accordingly,
288 univariate analyses further revealed high levels of relative importance (RI > 0.58) of the range expansion for
289 these traits (Table S3-S8). Thus, *Paramecium* from the range front populations generally had a 31% lower
290 population growth rate (Fig. 2C) and 54% higher equilibrium density (Fig. 2D) than *Paramecium* from the
291 range core. Similarly, the range front treatment was associated with 12% lower swimming speed (Fig.2E) and
292 23% more non-linear (i.e., tortuous) movement trajectories (Fig. 2F), compared to the range core treatment.

293 In long-term treatments with the parasite, phenotypic differentiation between infected and parasite-free
294 lines can be seen along the PC2 axis, and in part along the PC1 axis (Fig. 1, full vs empty dots). To some degree,
295 this parasite effect varied for range and core treatments, leading to overlap of the different treatment
296 combinations in Fig. 1. We identify three patterns. First, resistance and dispersal are the key traits associated
297 with the PC2 axis (Fig. 1), with trait trajectories indicating higher resistance for lines evolved with the parasite
298 and higher dispersal for parasite-free lines. Univariate analyses are in line with these trends. For resistance,
299 there was an interaction between range expansion and parasitism (Table 2 and Table S4; RI interaction =
300 0.42). Thus, the presence of parasite tended to increase resistance in the range front treatment (+15%), but
301 less so in core treatment (Fig. 2B) compared to the unexposed evolved counterparts (Fig. 2B). For dispersal,
302 there was a main effect of parasite treatment, with a generally lower dispersal of *Paramecium* from infected
303 long-term populations in both range core and front treatments (Table 2 and Table S3; RI parasitism = 0.28;
304 Fig. 2A).

305 Second, the parasite long-term treatment further modified differences in demographic traits, as shown by
306 the partial separation of parasite and parasite-free treatments along the opposing r_0/ $\bar{N}$ trajectories in the
307 PCA (Fig. 1). Thus, univariate analyses indicate that *Paramecium* from infected populations tended to have
308 higher equilibrium density (Fig. 2D) and lower growth rate (Fig. 2C) than those from parasite-free populations
309 (parasitism main effects, Table S5, S6). We also note that range front vs core differentiation in these traits
310 was less pronounced for infected populations, specifically for r_0 (RI range * parasitism interaction = 0.26,

Table 2). Third, the long-term presence of the parasite had no obvious effect on swimming behaviour (Fig.2E-F), leaving only the range treatment in the best model in the univariate analysis (RI > 0.93, Table S7, S8).

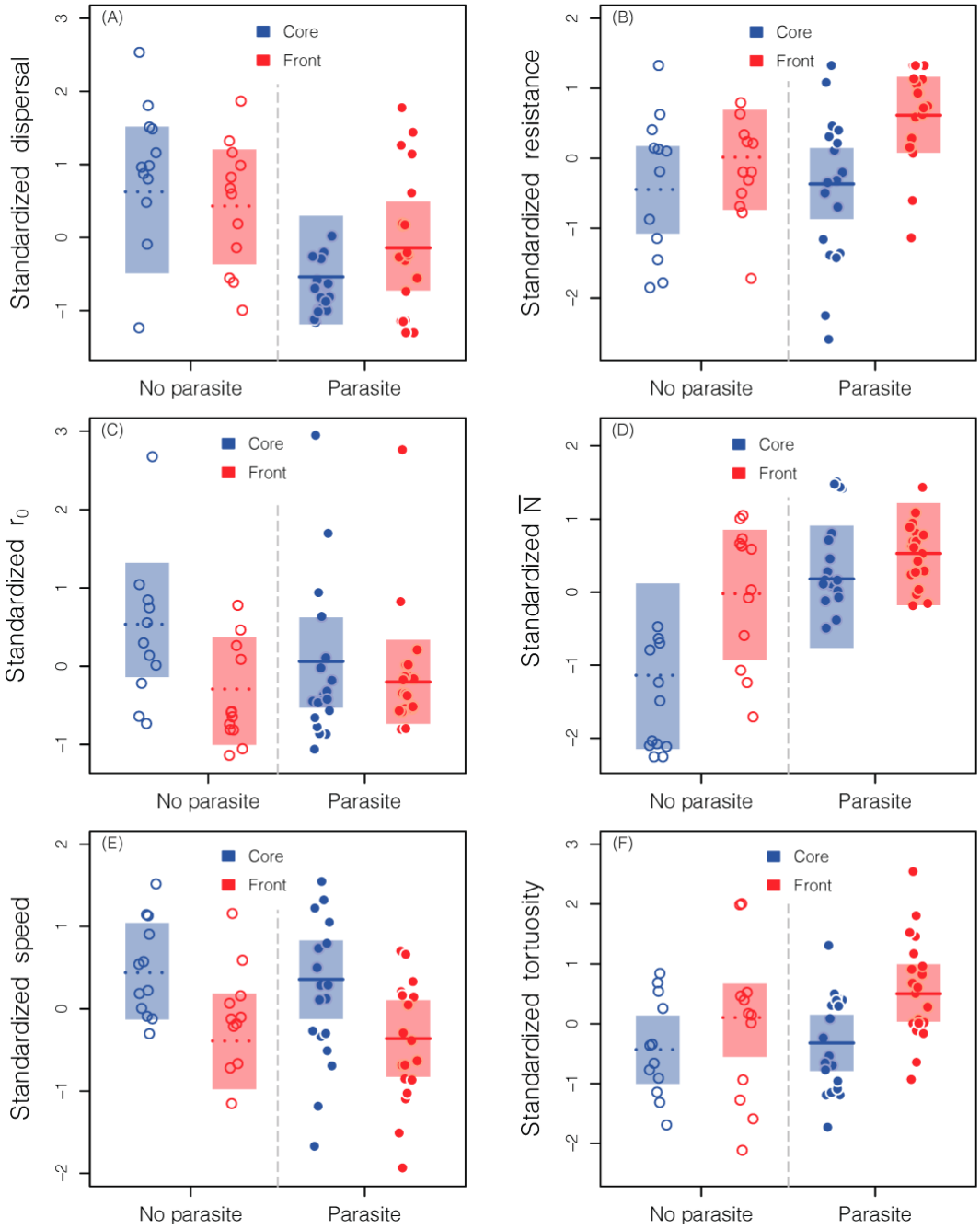

Figure 2 Standardized single trait panels of *P. caudatum* evolved in range core and range front treatments in the presence or absence of parasite: (A) dispersal, (B) resistance, (C) growth rate (r_0), (D) equilibrium density ($\overline{N}$), (E) swimming speed and (F) swimming tortuosity. For each panel, red and blue represent core and front treatment while the parasitism treatment is specified as follows: evolved in the presence of the parasite (full dots and lines) vs. parasite-free (empty dots and dashed lines). The points are the means for 63 monoclonal lines, isolated from a total of 16 long-term selection lines (for details, see text). The shaded areas and tick lines are the 95% compatibility interval and median of the averaged model of the posterior distributions.

Discussion

Eco-evolutionary dynamics in expanding edge populations can favour specific adaptations in dispersal capacity and reproductive strategies ("dispersal syndromes"), but still little is known about how these processes are modulated by interactions with natural enemies or parasites. This study investigated the interplay between spatial selection (range front vs core treatment) and parasite-mediated selection (absence vs presence of parasite) in a factorial experimental design. We found substantial divergence between our experimental range core and front populations, involving traits commonly known to produce “dispersal syndromes” (dispersal, population growth, movement behaviour). In addition, exposure to the parasite in infected populations brought into a play an additional trait (resistance), but also affected divergence in the other traits. In particular, populations evolved with the parasite were more resistant, but dispersed less than their uninfected counterparts. Three pairs of traits acted as opposing vectors in multi-trait space defining the phenotypic divergence between treatments: dispersal - resistance, population growth rate (r_0) - equilibrium density ($\overline{N}$) and swimming speed - tortuosity. Below we focus on the evolutionary forces driving these trait associations and discuss possible feedbacks on range expansion speed.

Resistance and dispersal: trade-off or concerted evolution?

Dispersal and resistance are among the most prominent traits expected to be under selection in range expansion and host-parasite coevolution contexts, respectively. In our study, we investigated their joint evolution. The PCA shows that the two traits have opposite signs, indicating a general negative relationship between dispersal and resistance. This negative association further scales up to the “parasite treatment” level (Fig. 2A, B), suggesting that parasite-mediated selection for increased resistance is accompanied by a decrease in dispersal. This general pattern was most obvious for populations in the range front treatment (panels on the right in Fig. 2A, B), for which we also detected a clear negative quasi-genetic (i.e., across monoclonal lines) correlation between the two traits (Table S9).

Previous work in our study system provided evidence for ample naturally occurring genetic variation in both resistance and dispersal [54,68], and both traits readily evolve under experimental conditions [55,57]. The genetic basis of the two traits is unknown, but we speculate that a trade-off could result from energy constraints arising from mounting an effective (constitutive) defence against the parasite, and/or from concomitant behavioural change. For example, the filter-feeding paramecia become infected when they ingest infectious spores together with other food particles. Hence, contact rates with the parasite may be reduced via reduced feeding activity. Such behavioural aspects of resistance may also include altered swimming behaviour, which can, in turn, affect dispersal (see below).

Even though resistance [69] and dispersal [70] are usually considered costly traits, we do not necessarily always expect trade-offs to evolve. In certain bacteria, cell surface modification conferring resistance to

354 bacteriophages leads to reduced motility [71,72]. Experiments also demonstrated that phage selects for
355 increased bacterial dispersal [71,73]. However, the link between dispersal and resistance was not clear,
356 implying that the two traits evolved independently. This suggests that, apart from mechanical or physiological
357 constraints, the emergence of evolutionary trade-offs also depends on the underlying genetic architecture
358 and relationships with fitness, or on the environmental conditions [45,54,74,75].

359 Finally, we would like to highlight that trade-offs can be a matter of perspective. A (genetic) trade-off with
360 resistance indeed suggests that parasites constrain the evolution of dispersal syndromes at the range front.
361 Yet, if we compare the two traits between range core and front treatments (rather than between parasite /
362 no parasite treatments), their association is positive: infected front populations have both higher resistance
363 and higher dispersal, when compared with the corresponding core populations (Fig. 2A, B, right panels). In
364 fact, this pattern matches findings for natural populations of the invasive cane toad, where front populations
365 show both higher resistance to lungworm parasites and larger dispersal-related morphological traits [32,41].
366 From these observations, we would conclude that resistance and dispersal can evolve concomitantly at the
367 invasion front, despite an inherent trade-off between the two traits. It could be the consequence of spatial
368 sorting, putting together variants with generally high levels of resistance and dispersal. In natural systems,
369 similar patterns can be driven by stressful range front environments causing stronger immune responses
370 [76,77].

371

372 **Parasitism exacerbates r_0 - $\bar{N}$ trade-off, but reduces range core-front divergence**

373 On the demographic axis of the multi-trait space, we found opposing directions for equilibrium density ($\bar{N}$)
374 and population growth rate (r_0) along the first PC axis, indicating a trade-off typical of classic r-K selection
375 theory (Fig. 1). This axis also separated populations from the range treatment front (high $\bar{N}$, low r_0) and range
376 core populations (low $\bar{N}$, high r_0). This pattern seems to contradict common ideas about dispersal syndrome
377 evolution (Burton et al. 2010), predicting competitive strategies in the core (high K or $\bar{N}$) and opportunistic
378 strategies at range fronts (high r_0). However, in our system as well as in another protist, competitive ability
379 is characterised by growth rate, rather than equilibrium density [57,59]. Thus, if food bacteria are a slowly
380 regrowing resource, rapacious high-growth protists are favoured in the core treatment and more slowly
381 growing variants at the front [59]. Comparative evidence suggests that this may actually be a widespread
382 pattern [78].

383 As in the previous section, parasite effects on these demographic traits are a matter of perspective. On the
384 one hand, the r_0 - $\bar{N}$ trade-off is more pronounced for populations evolving with the parasite than for
385 parasite-free populations. This trend appears relatively weak for overall treatment means (Fig. 2C, D), but is

386 well supported by supplementary analysis of correlations across monoclonal lines within treatments,
387 showing consistent negative r_0 - $\bar{N}$ correlations for the parasite treatment (Table S9). Possibly, this pattern
388 reflects indirect responses to selection on resistance, via costs of resistance, acting on demographic traits
389 [79]. On the other hand, the presence of the parasite decreased the trait differences between range core and
390 front treatments, when compared to the parasite-free treatments (Fig. 2C, D). This equalising tendency might
391 mean that the parasite makes demographic conditions in core and front populations more similar, and/or
392 that potential general indirect effects of parasite-mediated selection partly override spatial selection on
393 growth traits.

394 **Range expansion, but not parasitism influences swimming behaviour**

395 Our data show that Paramecium can (evolve to) swim either straight and fast or more slowly and take more
396 turns (Fig. 1). *Paramecium* from the range front treatment were clearly more of the slow type, consistent
397 with previous observation [57]. This contradicts results in a very similar experiment with another ciliate [59]
398 and observations in other biological systems, where populations at the range front show enhanced
399 movement ability [34,37]. In our case, speed reduction was associated with increased swimming tortuosity.
400 This latter tendency to change directions while swimming could represent an exploratory behaviour that
401 might influence the probability of finding the dispersal corridors in our connected microcosms. While our
402 range selection treatment had a strong impact on movement behaviour, there was no discernible effect of
403 the parasite treatment. Thus, unlike for the other trait pairs, parasite-mediated selection does not seem to
404 play a role in shaping the evolution of these traits. As stand-alone traits, speed and tortuosity are only weakly
405 correlated with dispersal (Table S9), suggesting that the effect of parasite treatment on dispersal must
406 operate through other aspects of movement.

407 **From eco to evo and back: Is the evolution with a parasite slowing down range expansions?**

408 The evolution of dispersal syndromes typically produces ecological feedbacks that speed up range expansions
409 [4]. Parasites, in contrast, may keep in check host populations and thereby limit or slow down range fronts,
410 as generically shown for interspecific (antagonistic) interactions [5,11,80]. Parasites may indeed modify
411 ecological dynamics by affecting host demography and dispersal during a range expansion, and consequently
412 alter the strength or sign selection on these traits. Moreover, parasite resistance to is yet another trait under
413 selection. The main purpose of this study was to investigate such eco-to-evo feedbacks and assess the
414 possible impact of a parasite on the evolutionary trajectories of dispersal syndromes. The open question is
415 how these evolutionary changes in turn feedback on the ecological dynamics of a range expansion, regarding
416 the demography, dispersal or expansion speed. One of our main findings is that the presence of the parasite
417 in the range front treatment favours higher resistance, but also leads to lower dispersal, when compared to
418 the parasite-free treatment (Fig. 2A, B). Thus, an intuitive prediction is that evolution with the parasite slows
419 down range expansion speed, due to this resistance - dispersal trade-off. To apply this prediction to natural

420 systems is difficult because these might rarely be replicated with and without parasites. However, as already
421 discussed above for the cane toad example, there are cases where resistance evolution does occur at the
422 range expansion front [41]. And even though it is unknown how the resistance evolution in the toad is
423 correlated with dispersal traits, it seems obvious that, in the face of a detrimental parasite (a lung worm),
424 having the resistance will benefit the range expansion more than not having it [12], at least as long as
425 parasites equally infect high- and low-dispersal individuals, preventing escape into enemy-free space.

426 Beyond these simple considerations, however, answers may be more complex [81], if we add a multi-trait
427 perspective. As we have shown here, parasite-mediated selection may affect some dispersal syndrome
428 components, but not others, or even modify the correlation between these components. Moreover, a full
429 picture would require measurements of growth, dispersal, and movement in the presence of infection,
430 thereby integrating aspects or virulence / tolerance or context-dependent dispersal [53,54]. In a next step
431 towards a more comprehensive understanding of eco-evo feedbacks, future experiments can use multi-
432 microcosm landscapes to actually measure range expansion speeds for the different types of evolved hosts,
433 with and without parasite. Ideally, this would be accompanied by theory exploring the simultaneous
434 evolution of dispersal and interaction traits [82] or accounting for additional factors, such as parasite
435 evolution [53], dispersal plasticity [45,54] or the general upregulation of immune responses, known to occur
436 during range expansion [76,77].

437 **Conclusion**

438 Our selection experiment illustrates the possible impact of biotic interactions on evolutionary trajectories
439 during range expansions. Parasite-mediated selection changed the structure of dispersal syndromes, shaping
440 the phenotypic divergence between front and core populations for multiple traits, including dispersal, life-
441 history and resistance. Here we focused on the single-sided host evolution, but dispersal syndromes also
442 evolved in the parasite [53]. It could mean that our observed host changes may have an additional
443 coevolutionary component. This may further complexify the interplay between spatial selection and biotic
444 (co-)evolution, and make it even more difficult to predict the accompanying ecological feedbacks on range
445 expansion dynamics or disease spread. Replicated range expansions under laboratory conditions represent
446 one tool to disentangle these processes. Although being simplified abstractions of the real world, such
447 experiments may also provide baseline information for applied issues of biocontrol or the monitoring of
448 emerging diseases.

449 ## Ethics

450 Not applicable

Data accessibility

The data from this study are available at https://doi.org/10.5281/zenodo.7123494

Authors' contributions

OK, LN and GZ conceived the study. GZ, LN, MH, EAF, and OK designed the experiments. GZ, LN, CGB and OK performed the experimental work. GZ, LN, OK and EAF performed the statistical analysis. All authors interpreted the results. GZ and OK wrote the first draft of the manuscript and all authors commented on the final version.

Competing interests

The authors declare no competing financial interests.

Funding

This work was funded by the Swiss National Science Foundation (grant no. P2NEP3_184489) to GZ and by the 2019 Godfrey Hewitt Mobility Award granted to LN by ESEB.

Acknowledgements

This is publication ISEM-YYYY-XXX of the Institut des Sciences de l'Evolution - Montpellier.

References

1. Parmesan C, Yohe G. 2003 A globally coherent fingerprint of climate change impacts across natural systems. *Nature* **421**, 37–42. (doi:10.1038/nature01286)

2. Thomas CD *et al.* 2004 Extinction risk from climate change. *Nature* **427**, 145–148. (doi:10.1038/nature02121)

3. Kubisch A, Holt RD, Poethke H-J, Fronhofer EA. 2014 Where am I and why? Synthesizing range biology and the eco-evolutionary dynamics of dispersal. *Oikos* **123**, 5–22. (doi:10.1111/j.1600-0706.2013.00706.x)

4. Miller TEX *et al.* 2020 Eco-evolutionary dynamics of range expansion. *Ecology* **101**, e03139. (doi:10.1002/ecy.3139)

5. Kubisch A, Degen T, Hovestadt T, Poethke HJ. 2013 Predicting range shifts under global change: the balance between local adaptation and dispersal. *Ecography* **36**, 873–882. (doi:10.1111/j.1600-0587.2012.00062.x)

6. Legault G, Bitters ME, Hastings A, Melbourne BA. 2020 Interspecific competition slows range expansion and shapes range boundaries. *Proc. Natl. Acad. Sci.* **117**, 26854–26860. (doi:10.1073/pnas.2009701117)

481 7. Bowler DE *et al.* 2020 Mapping human pressures on biodiversity across the planet uncovers
482 anthropogenic threat complexes. *People Nat.* **2**, 380–394. (doi:10.1002/pan3.10071)

483 8. Morales-Castilla I, Pappalardo P, Farrell MJ, Aguirre AA, Huang S, Gehman A-LM, Dallas T, Gravel D,
484 Davies TJ. 2021 Forecasting parasite sharing under climate change. *Philos. Trans. R. Soc. B Biol. Sci.* **376**,
485 20200360. (doi:10.1098/rstb.2020.0360)

486 9. Hochberg ME, Ives AR. 1999 Can natural enemies enforce geographical range limits? *Ecography* **22**,
487 268–276. (doi:10.1111/j.1600-0587.1999.tb00502.x)

488 10. Holt RD, Keitt TH. 2000 Alternative causes for range limits: a metapopulation perspective. *Ecol. Lett.* **3**,
489 41–47. (doi:10.1046/j.1461-0248.2000.00116.x)

490 11. Price TD, Kirkpatrick M. 2009 Evolutionarily stable range limits set by interspecific competition. *Proc. R.*
491 *Soc. B Biol. Sci.* **276**, 1429–1434. (doi:10.1098/rspb.2008.1199)

492 12. Finnerty PB, Shine R, Brown GP. 2018 The costs of parasite infection: Effects of removing lungworms on
493 performance, growth and survival of free-ranging cane toads. *Funct. Ecol.* **32**, 402–415.
494 (doi:10.1111/1365-2435.12992)

495 13. Kelehear C, Webb JK, Shine R. 2009 Rhabdias pseudosphaerocephala infection in Bufo marinus: lung
496 nematodes reduce viability of metamorph cane toads. *Parasitology* **136**, 919–927.
497 (doi:10.1017/S0031182009006325)

498 14. Antonovics J, Edwards M. 2011 Spatio-temporal dynamics of bumblebee nest parasites (Bombus
499 subgenus Psythirus ssp.) and their hosts (Bombus spp.). *J. Anim. Ecol.* **80**, 999–1011.
500 (doi:10.1111/j.1365-2656.2011.01846.x)

501 15. Bradley CA, Altizer S. 2005 Parasites hinder monarch butterfly flight: implications for disease spread in
502 migratory hosts: Parasites and monarch flight. *Ecol. Lett.* **8**, 290–300. (doi:10.1111/j.1461-
503 0248.2005.00722.x)

504 16. Briers RA. 2003 Range limits and parasite prevalence in a freshwater snail. *Proc. R. Soc. Lond. B Biol. Sci.*
505 **270**, S178–S180. (doi:10.1098/rsbl.2003.0046)

506 17. Dunn AM *et al.* 2012 Indirect effects of parasites in invasions. *Funct. Ecol.* **26**, 1262–1274.
507 (doi:10.1111/j.1365-2435.2012.02041.x)

508 18. Strauss A, White A, Boots M. 2012 Invading with biological weapons: the importance of disease-
509 mediated invasions. *Funct. Ecol.* **26**, 1249–1261. (doi:10.1111/1365-2435.12011)

510 19. Combe M, Gozlan RE. 2018 The rise of the rosette agent in Europe: An epidemiological enigma.
511 *Transbound. Emerg. Dis.* **65**, 1474–1481. (doi:10.1111/tbed.13001)

512 20. Miller MA, Kinsella JM, Snow RW, Hayes MM, Falk BG, Reed RN, Mazzotti FJ, Guyer C, Romagosa CM.
513 2018 Parasite spillover: indirect effects of invasive Burmese pythons. *Ecol. Evol.* **8**, 830–840.
514 (doi:10.1002/ece3.3557)

515 21. Halloran ME, Longini IM. 2014 Emerging, evolving, and established infectious diseases and
516 interventions. *Science* **345**, 1292–1294. (doi:10.1126/science.1254166)

517 22. Smith KF, Goldberg M, Rosenthal S, Carlson L, Chen J, Chen C, Ramachandran S. 2014 Global rise in
518 human infectious disease outbreaks. *J. R. Soc. Interface* **11**, 20140950. (doi:10.1098/rsif.2014.0950)

23. Poulin R. 2017 Invasion ecology meets parasitology: Advances and challenges. *Int. J. Parasitol. Parasites Wildl.* **6**, 361–363. (doi:10.1016/j.ijppaw.2017.03.006)

24. Crowley SL, Hinchliffe S, McDonald RA. 2017 Conflict in invasive species management. *Front. Ecol. Environ.* **15**, 133–141. (doi:10.1002/fee.1471)

25. Clobert J, Galliard J-FL, Cote J, Meylan S, Massot M. 2009 Informed dispersal, heterogeneity in animal dispersal syndromes and the dynamics of spatially structured populations. *Ecol. Lett.* **12**, 197–209. (doi:10.1111/j.1461-0248.2008.01267.x)

26. Cote J, Bestion E, Jacob S, Travis J, Legrand D, Baguette M. 2017 Evolution of dispersal strategies and dispersal syndromes in fragmented landscapes. *ECOGRAPHY* **40**, 56–73. (doi:10.1111/ecog.02538)

27. Shine R, Brown GP, Phillips BL. 2011 An evolutionary process that assembles phenotypes through space rather than through time. *Proc. Natl. Acad. Sci.* **108**, 5708–5711. (doi:10.1073/pnas.1018989108)

28. Kubisch A, Fronhofer EA, Poethke HJ, Hovestadt T. 2013 Kin Competition as a Major Driving Force for Invasions. *Am. Nat.* **181**, 700–706. (doi:10.1086/670008)

29. Saastamoinen M *et al.* 2018 Genetics of dispersal. *Biol. Rev.* **93**, 574–599. (doi:10.1111/brv.12356)

30. Chuang A, Peterson CR. 2016 Expanding population edges: theories, traits, and trade-offs. *Glob. Change Biol.* **22**, 494–512. (doi:10.1111/gcb.13107)

31. Fjerdingstad EJ, Schtickzelle N, Manhes P, Gutierrez A, Clobert J. 2007 Evolution of dispersal and life history strategies – Tetrahymena ciliates. *BMC Evol. Biol.* **7**, 133. (doi:10.1186/1471-2148-7-133)

32. Brown GP, Phillips BL, Shine R. 2014 The straight and narrow path: the evolution of straight-line dispersal at a cane toad invasion front. *Proc. R. Soc. B Biol. Sci.* **281**, 20141385. (doi:10.1098/rspb.2014.1385)

33. Perkins TA, Phillips BL, Baskett ML, Hastings A. 2013 Evolution of dispersal and life history interact to drive accelerating spread of an invasive species. *Ecol. Lett.* **16**, 1079–1087. (doi:10.1111/ele.12136)

34. Phillips BL, Brown GP, Webb JK, Shine R. 2006 Invasion and the evolution of speed in toads. *Nature* **439**, 803–803. (doi:10.1038/439803a)

35. Lombaert E, Estoup A, Facon B, Joubard B, Grégoire J-C, Jannin A, Blin A, Guillemaud T. 2014 Rapid increase in dispersal during range expansion in the invasive ladybird *Harmonia axyridis*. *J. Evol. Biol.* **27**, 508–517. (doi:10.1111/jeb.12316)

36. Szűcs M, Vahsen ML, Melbourne BA, Hoover C, Weiss-Lehman C, Hufbauer RA. 2017 Rapid adaptive evolution in novel environments acts as an architect of population range expansion. *Proc. Natl. Acad. Sci.* **114**, 13501–13506. (doi:10.1073/pnas.1712934114)

37. Weiss-Lehman C, Hufbauer RA, Melbourne BA. 2017 Rapid trait evolution drives increased speed and variance in experimental range expansions. *Nat. Commun.* **8**, 1–7. (doi:10.1038/ncomms14303)

38. Williams JL, Kendall BE, Levine JM. 2016 Rapid evolution accelerates plant population spread in fragmented experimental landscapes. *Science* **353**, 482–485. (doi:10.1126/science.aaf6268)

39. Lion S, Gandon S. 2015 Evolution of spatially structured host-parasite interactions. *J. Evol. Biol.* **28**, 10–28. (doi:10.1111/jeb.12551)

40. Parratt SR, Numminen E, Laine A-L. 2016 Infectious Disease Dynamics in Heterogeneous Landscapes. *Annu. Rev. Ecol. Evol. Syst.* **47**, 283–306. (doi:10.1146/annurev-ecolsys-121415-032321)

41. Mayer M, Shine R, Brown GP. 2021 Rapid divergence of parasite infectivity and host resistance during a biological invasion. *Biol. J. Linn. Soc.* **132**, 861–871. (doi:10.1093/biolinnean/blaa229)

42. Schlippe Justicia L, Mayer M, Shine R, Shilton C, Brown GP. 2022 Divergence in host–parasite interactions during the cane toad's invasion of Australia. *Ecol. Evol.* **12**, e9220. (doi:10.1002/ece3.9220)

43. Chaianunporn T, Hovestadt T. 2012 Concurrent evolution of random dispersal and habitat niche width in host-parasitoid systems. *Ecol. Model.* **247**, 241–250. (doi:10.1016/j.ecolmodel.2012.09.005)

44. Chaianunporn T, Hovestadt T. 2012 Evolution of dispersal in metacommunities of interacting species. *J. Evol. Biol.* **25**, 2511–2525. (doi:10.1111/j.1420-9101.2012.02620.x)

45. Deshpande JN, Kaltz O, Fronhofer EA. 2021 Host-parasite dynamics set the ecological theatre for the evolution of state- and context-dependent dispersal in hosts. *OIKOS* **130**, 121–132. (doi:10.1111/oik.07512)

46. Luong LT, Polak M. 2007 Costs of Resistance in the Drosophila–Macrocheles System: A Negative Genetic Correlation Between Ectoparasite Resistance and Reproduction. *Evolution* **61**, 1391–1402. (doi:10.1111/j.1558-5646.2007.00116.x)

47. Sgrò CM, Hoffmann AA. 2004 Genetic correlations, tradeoffs and environmental variation. *Heredity* **93**, 241–248. (doi:10.1038/sj.hdy.6800532)

48. Duffy MA, Forde SE. 2009 Ecological feedbacks and the evolution of resistance. *J. Anim. Ecol.* **78**, 1106–1112. (doi:10.1111/j.1365-2656.2009.01568.x)

49. Kraaijeveld AR, Godfray HCJ. 1997 Trade-off between parasitoid resistance and larval competitive ability in Drosophila melanogaster. *Nature* **389**, 278–280. (doi:10.1038/38483)

50. Wichterman R. 1986 *The Biology of Paramecium*. Springer US. (doi:10.1007/978-1-4757-0372-6)

51. Fokin SI, Görtz H-D. 2009 Diversity of Holospora Bacteria in Paramecium and Their Characterization. In *Endosymbionts in Paramecium* (ed M Fujishima), pp. 161–199. Berlin, Heidelberg: Springer. (doi:10.1007/978-3-540-92677-1_7)

52. Fellous S, Quillery E, Duncan AB, Kaltz O. 2011 Parasitic infection reduces dispersal of ciliate host. *Biol. Lett.* **7**, 327–329. (doi:10.1098/rsbl.2010.0862)

53. Nørgaard LS, Zilio G, Saade C, Gougat-Barbera C, Hall MD, Fronhofer EA, Kaltz O. 2021 An evolutionary trade-off between parasite virulence and dispersal at experimental invasion fronts. *Ecol. Lett.* , ele.13692. (doi:10.1111/ele.13692)

54. Zilio G, Nørgaard LS, Petrucci G, Zeballos N, Gougat-Barbera C, Fronhofer EA, Kaltz O. 2021 Parasitism and host dispersal plasticity in an aquatic model system. *J. Evol. Biol.* , jeb.13893. (doi:10.1111/jeb.13893)

55. Lohse K, Gutierrez A, Kaltz O. 2006 Experimental evolution of resistance in Paramecium caudatum against the bacterial parasite Holospora undulata. *Evolution* **60**, 1177–1186. (doi:10.1111/j.0014-3820.2006.tb01196.x)

56. Duncan AB, Fellous S, Kaltz O. 2011 Temporal variation in temperature determines disease spread and maintenance in Paramecium microcosm populations. *Proc. R. Soc. B Biol. Sci.* **278**, 3412–3420. (doi:10.1098/rspb.2011.0287)

57. Zilio G, Krenek S, Gougat-Barbera C, Fronhofer EA, Kaltz O. 2022 Predicting evolution in experimental range expansions of an aquatic model system. , 2022.01.20.477128. (doi:10.1101/2022.01.20.477128)

58. Rosenbaum B, Raatz M, Weithoff G, Fussmann GF, Gaedke U. 2019 Estimating Parameters From Multiple Time Series of Population Dynamics Using Bayesian Inference. *Front. Ecol. Evol.* **6**. (doi:10.3389/fevo.2018.00234)

59. Fronhofer EA, Altermatt F. 2015 Eco-evolutionary feedbacks during experimental range expansions. *Nat. Commun.* **6**, 6844. (doi:10.1038/ncomms7844)

60. Pennekamp F, Schtickzelle N, Petchey OL. 2015 BEMOVI, software for extracting behavior and morphology from videos, illustrated with analyses of microbes. *Ecol. Evol.* **5**, 2584–2595. (doi:10.1002/ece3.1529)

61. R Core Team. In press. R: A language and environment for statistical computing. *R Found. Stat. Comput. Vienna Austria URL HttpswwwR-Proj.*

62. Stan Development Team. 2022 RStan: the R interface to Stan. (doi:https://mc-stan.org/)

63. Bürkner P-C. 2021 Bayesian Item Response Modeling in R with brms and Stan. *J. Stat. Softw.* **100**, 1–54. (doi:10.18637/jss.v100.i05)

64. McElreath, R. 2020 *Statistical rethinking: A Bayesian course with examples in R and Stan.* 2nd edn. Chapman and Hall/CRC.

65. Buuren S van, Groothuis-Oudshoorn K. 2011 mice: Multivariate Imputation by Chained Equations in R. *J. Stat. Softw.* **45**, 1–67. (doi:10.18637/jss.v045.i03)

66. Watanabe S. 2010 Asymptotic Equivalence of Bayes Cross Validation and Widely Applicable Information Criterion in Singular Learning Theory. *J. Mach. Learn. Res.* **11**, 3571–3594.

67. Gelman A, Hwang J, Vehtari A. 2014 Understanding predictive information criteria for Bayesian models. *Stat. Comput.* **24**, 997–1016. (doi:10.1007/s11222-013-9416-2)

68. Weiler J, Zilio G, Zeballos N, Nørgaard L, Conce Alberto WD, Krenek S, Kaltz O, Bright L. 2020 Among-Strain Variation in Resistance of Paramecium caudatum to the Endonuclear Parasite Holospora undulata: Geographic and Lineage-Specific Patterns. *Front. Microbiol.* **11**, 603046. (doi:10.3389/fmicb.2020.603046)

69. Schmid-Hempel P. 2003 Variation in immune defence as a question of evolutionary ecology. *Proc. R. Soc. B Biol. Sci.* **270**, 357–366. (doi:10.1098/rspb.2002.2265)

70. Bonte D *et al.* 2012 Costs of dispersal. *Biol. Rev.* **87**, 290–312. (doi:10.1111/j.1469-185X.2011.00201.x)

71. Koskella B, Taylor TB, Bates J, Buckling A. 2011 Using experimental evolution to explore natural patterns between bacterial motility and resistance to bacteriophages. *ISME J.* **5**, 1809–1817. (doi:10.1038/ismej.2011.47)

629 72. Whitchurch CB, Mattick JS. 1994 Escherichia coli contains a set of genes homologous to those involved
630 in protein secretion, DNA uptake and the assembly of type-4 fimbriae in other bacteria. *Gene* **150**, 9–
631 15. (doi:10.1016/0378-1119(94)90851-6)

632 73. Taylor TB, Buckling A. 2013 Bacterial motility confers fitness advantage in the presence of phages. *J.*
633 *Evol. Biol.* **26**, 2154–2160. (doi:10.1111/jeb.12214)

634 74. Boots M. 2011 The Evolution of Resistance to a Parasite Is Determined by Resources. *Am. Nat.* **178**,
635 214–220. (doi:10.1086/660833)

636 75. Meaden S, Paszkiewicz K, Koskella B. 2015 The cost of phage resistance in a plant pathogenic bacterium
637 is context-dependent. *Evol. Int. J. Org. Evol.* **69**, 1321–1328. (doi:10.1111/evo.12652)

638 76. Gardner ST, Assis VR, Smith KM, Appel AG, Mendonça MT. 2020 Innate immunity of Florida cane toads:
639 how dispersal has affected physiological responses to LPS. *J. Comp. Physiol. [B]* **190**, 317–327.
640 (doi:10.1007/s00360-020-01272-7)

641 77. Diagne C *et al.* 2017 Contemporary variations of immune responsiveness during range expansion of
642 two invasive rodents in Senegal. *Oikos* **126**, 435–446. (doi:10.1111/oik.03470)

643 78. Dallas T, Park AW, Drake JM. 2017 Predicting cryptic links in host-parasite networks. *PLOS Comput. Biol.*
644 **13**. (doi:10.1371/journal.pcbi.1005557)

645 79. Duncan AB, Fellous S, Kaltz O. 2011 Reverse Evolution: Selection Against Costly Resistance in Disease-
646 Free Microcosm Populations of Paramecium Caudatum. *Evolution* **65**, 3462–3474. (doi:10.1111/j.1558-
647 5646.2011.01388.x)

648 80. Moorcroft PR, Pacala SW, Lewis MA. 2006 Potential role of natural enemies during tree range
649 expansions following climate change. *J. Theor. Biol.* **241**, 601–616. (doi:10.1016/j.jtbi.2005.12.019)

650 81. Barnett LK, Phillips BL, Heath ACG, Coates A, Hoskin CJ. 2018 The impact of parasites during range
651 expansion of an invasive gecko. *Parasitology* **145**, 1400–1409. (doi:10.1017/S003118201800015X)

652 82. Drown DM, Dybdahl MF, Gomulkiewicz R. 2013 Consumer–Resource Interactions and the Evolution of
653 Migration. *Evolution* **67**, 3290–3304. (doi:10.1111/evo.12194)

654

655

656

657

658

659

660

661

662

663

664 # Supplementary Information

665 **S1 Dispersal systems**

666 We first filled the two-patch system with 9.5 mL of fresh growth medium and we then closed the corridor
667 with a clamp. Secondly, we filled to 13 mL one of the two tubes, the core patch, using the paramecia and
668 medium from an experimental selection line. The second tube, the front patch, was filled to 13 mL with fresh
669 growth medium, and thus resulted empty at this stage. Thirdly, we removed the clamp and opened the
670 corridor allowing the paramecia to actively disperse and swim from core to front patch or to stay in the core.
671 After three hours, we closed the corridor tube and we estimated the population density by taking a 200 µL
672 sample from core and front patch and counting the number of individuals under a dissecting microscope.

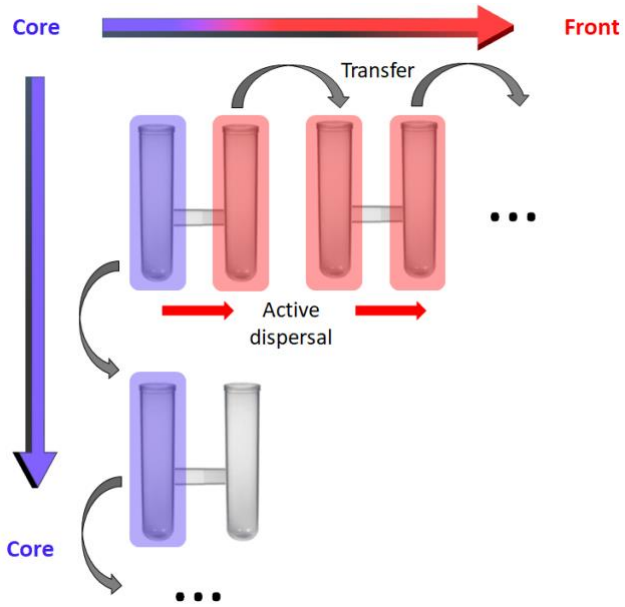

673

674 **Figure S1** Dispersal arenas used for the range expansion dynamics with representation of how the front treatment was propagated.
675 The arenas were composed from two patches (core and front) interconnected by 5-cm silicon tubing serving as a corridor. The
676 *paramecia* could displace from core to front patch through active dispersal once we removed the clamp blocking the corridor. In the
677 long-term experiment, we alternated short episodes of dispersal (3h) with periods of population growth and maintenance (1 week =
678 1 cycle). The same protocol was repeated for the core and front treatment with the parasite.

679

680 **S2 Extraction protocol**

681 Inocula were prepared concentrating by centrifugation infected paramecia (35000 RPM for 20 minutes) in
682 Falcon tubes filled with 15 mL of medium. After removing the supernatant, the concentrated individuals were
683 transferred into 1.5 mL Eppendorf tubes containing 1 mm glass beads, and they were vortexed and crushed
684 using a Qiagen TissuLyser (1.45 minutes at 30 oscillation frequency). The released infectious forms were then

counted using a hemocytometer at 200 x magnification under a microscope (Leica DM LB2), and their concentration was adjusted with sterile water.

S3 Design phenotypic trait assays

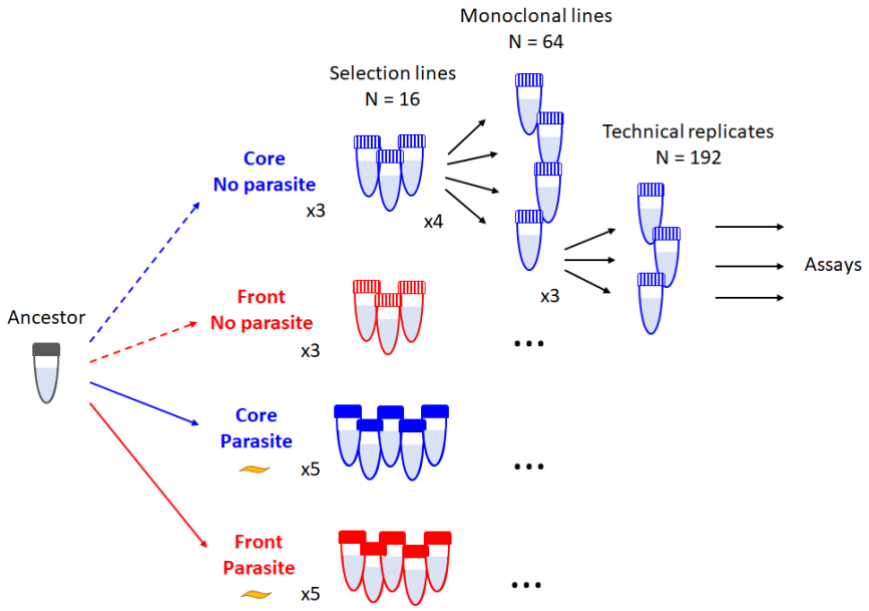

Figure S3 Experimental design of the phenotypic trait assays (16 x 4 x 3 tubes). Some technical replicates were lost during the manipulation, and the final number was 180. This corresponded to the total of 63 monoclonal lines that were used in the analysis.

703 **S4 Long-Term cycles**

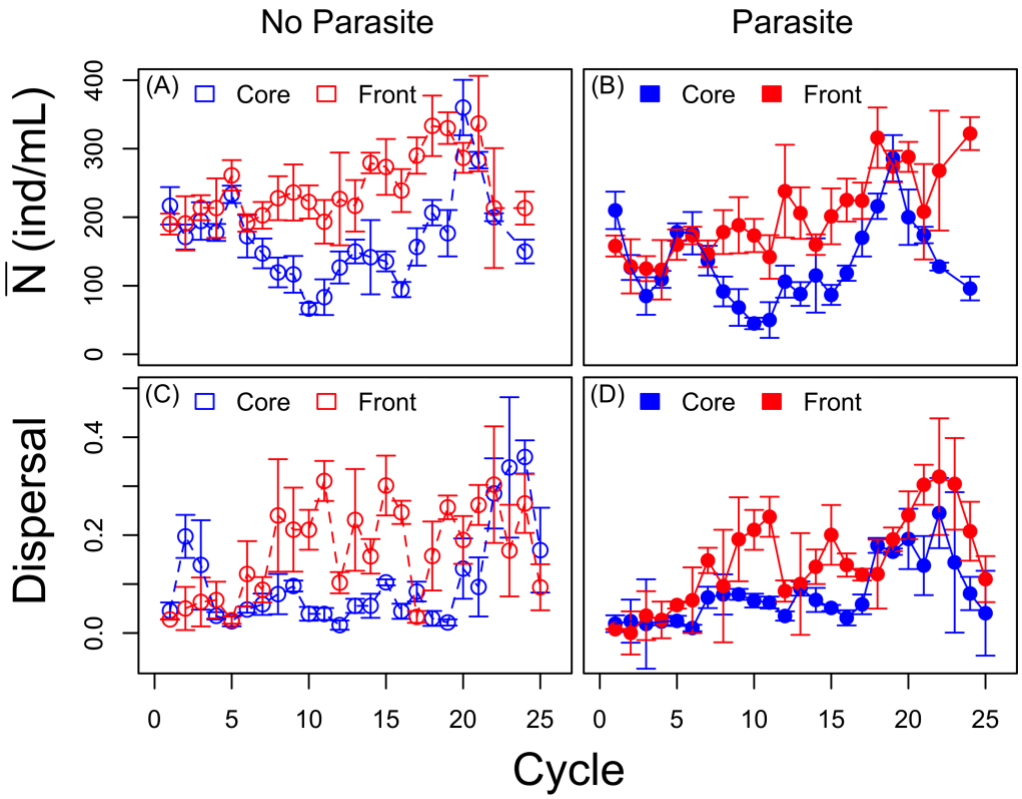

704

705 **Figure S4** Density (individuals per mL) and dispersal (proportion of individuals dispersing in 3 hours) dynamics during the first 25
706 cycles of the long-term range expansion experiment for (A)-(C) populations not infected (empty symbols), and (B)-(D) infected (full
707 symbols). Each point is the selection lines mean with the standard error, core treatment is in blue and front treatment in red.

708

709 **S5 Dispersal rate**

710 We followed a similar procedure to what was previously described for the dispersal systems. In short, we
711 filled the 3-patch systems with 40 mL of fresh growth medium, we closed the two corridors with clamps, and
712 then added the entire 25 mL of the final tube to the central compartment. Left and right tubes were filled
713 with fresh growth medium to have the same amount of volume of the central tube, then the corridors were
714 opened. We allowed the paramecia to actively disperse in both directions for three hours before closing the
715 dispersal corridors again. We sampled 500 µL from the core patch, 3 mL from both front patches and we
716 estimated population densities.

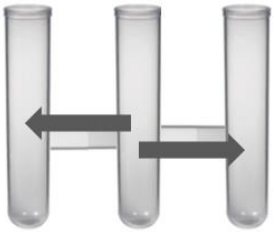

Figure S5 Linear 3-patch arena used to measure dispersal rate after evolution (3 interconnected 50 mL Falcon tubes). The Paramecium dispersed from the middle to the two outer tubes (arrows). Similarly to the protocol used during the long-term experiment, we opened the corridors for 3 h. Dispersal rates were estimated by sampling and counting the Paramecium from the central tube (500 µl) and from the combined two outer tubes (3 mL). We did not control for the density of Paramecium placed in the middle tube of the dispersal arena. However, preliminary analysis showed no significant effect of density on dispersal rate ($F_{1,54}$= 0.69, n.s.), and the covariate was therefore omitted from further analyses.

Tables

Table S1. PCA Eigenvalues and variance explained. PCA based on values for 6 traits measured for 63 monoclonal lines from 4 long-term treatments (for details, see main text).

	PC1	PC2	PC3	PC4	PC5	PC6
Eigenvalues	2.0876	1.3090	1.0711	0.6416	0.5950	0.2964
Proportion variance explained	0.3479	0.2182	0.1785	0.1070	0.0991	0.0492
Cumulative proportion	0.3479	0.5661	0.7446	0.8516	0.9507	1.0000

Table S2. Loading values of the PCA for 6 host traits.

	PC1	PC2	PC3	PC4	PC5	PC6
Dispersal	+0.0438	-0.7503	+0.0305	+0.0878	-0.6512	-0.0481
Resistance	-0.0789	+0.2485	+0.8531	+0.3932	-0.2049	+0.0860
Speed	+0.5669	+0.2951	+0.0632	-0.2034	-0.2756	-0.6855
Tortuosity	-0.5282	-0.3054	+0.2780	-0.1978	+0.3487	-0.6241
r_0	+0.4238	-0.2944	+0.4354	-0.5971	+0.2835	+0.3271
$\bar{N}$	-0.4601	+0.3288	+0.0162	-0.6328	-0.5057	+0.1537

Table S3. Single trait analysis of dispersal, testing effects of range expansion (front vs core) and parasitism (absence / presence of parasite) treatments. Rows are the different models; the best model is highlighted in bold. Columns are the explanatory variables included with the corresponding WAIC, standard error of the WAIC and WAIC weights for each model. The RI row indicates the relative importance of the explanatory variables.

	Range expansion	Parasitism	Range * Parasitism	WAIC	SE	WAIC weight
Model 1				155.6	11.9	0.14
Model 2		**X**		**154.2**	**12.7**	**0.28**
Model 3	X			156.0	11.9	0.11
Model 4	X	X		154.8	12.6	0.21
Model 5	X	X	X	154.3	12.7	0.26
RI	0.58	0.75	0.26			

Table S4. Single trait analysis of resistance, testing effects of range expansion (front vs core) and parasitism (absence / presence of parasite) treatments. Rows are the different models; the best model is highlighted in bold. Columns are the explanatory variables included with the corresponding WAIC, standard error of the WAIC and WAIC weights for each model. The RI row indicates the relative importance of the explanatory variables.

	Range expansion	Parasitism	Range * Parasitism	WAIC	SE	WAIC weight
Model 1				173.1	10.8	0.07
Model 2		X		173.7	11.1	0.05
Model 3	X			171.0	10.5	0.21
Model 4	X	X		170.7	11.1	0.24
Model 5	**X**	**X**	**X**	**169.6**	**11.0**	**0.42**
RI	0.87	0.71	0.42			

Table S5. Single trait analysis of r_0, testing effects of range expansion (front vs core) and parasitism (absence / presence of parasite) treatments. Rows are the different models; the best model is highlighted in bold. Columns are the explanatory variables included with the corresponding WAIC, standard error of the WAIC and WAIC weights for each model. The RI row indicates the relative importance of the explanatory variables.

	Range expansion	Parasitism	Range * Parasitism	WAIC	SE	WAIC weight
Model 1				181.7	20.1	0.17
Model 2		X		182.3	19.8	0.12
Model 3	X			180.8	19.7	0.26
Model 4	X	X		181.5	19.5	0.18
Model 5	**X**	**X**	**X**	**180.8**	**19.2**	**0.26**
RI	0.70	0.56	0.26			

Table S6. Single trait analysis of $\overline{N}$, testing effects of range expansion (front vs core) and parasitism (absence / presence of parasite) treatments. Rows are the different models; the best model is highlighted in bold. Columns are the explanatory variables included with the corresponding WAIC, standard error of the WAIC and WAIC weights for each model. The RI row indicates the relative importance of the explanatory variables.

	Range expansion	Parasitism	Range * Parasitism	WAIC	SE	WAIC weight
Model 1				98.4	14.2	0.18
Model 2		X		98.1	13.3	0.21
Model 3	X			98.5	14.4	0.17
Model 4	**X**	**X**		**97.9**	**13.4**	**0.23**
Model 5	X	X	X	98.0	13.8	0.22
RI	0.62	0.66	0.22			

767 **Table S7.** Single trait analysis of swimming speed, testing effects of range expansion (front vs core) and parasitism
768 (absence / presence of parasite) treatments. Rows are the different models; the best model is highlighted in bold.
769 Columns are the explanatory variables included with the corresponding WAIC, standard error of the WAIC and WAIC
770 weights for each model. The RI row indicates the relative importance of the explanatory variables.

	Range expansion	Parasitism	Range * Parasitism	WAIC	SE	WAIC weight
Model 1				182.4	19.3	0.04
Model 2		X		184.0	19.5	0.02
Model 3	**X**			**176.7**	**18.5**	**0.62**
Model 4	X	X		178.8	18.8	0.22
Model 5	X	X	X	180.4	18.5	0.10
RI	0.94	0.34	0.10			

771

772

773 **Table S8.** Single trait analysis of swimming tortuosity, testing effects of range expansion (front vs core) and parasitism
774 (absence / presence of parasite) treatments. Rows are the different models; the best model is highlighted in bold.
775 Columns are the explanatory variables included with the corresponding WAIC, standard error of the WAIC and WAIC
776 weights for each model. The RI row indicates the relative importance of the explanatory variables.

	Range expansion	Parasitism	Range * Parasitism	WAIC	SE	WAIC weight
Model 1				181.6	11.0	0.03
Model 2		X		182.1	11.0	0.02
Model 3	**X**			**176.5**	**11.3**	**0.39**
Model 4	X	X		176.8	10.9	0.34
Model 5	X	X	X	177.7	10.8	0.22
RI	0.95	0.56	0.22			

777

778

779

780

781

782

783

784 **Table S9** Mean correlation coefficients for selected pairs of host traits (± 95% compatibility intervals obtained from
785 posterior distributions).

Pair of traits	Range expansion	Parasitism	Mean correlation coefficient ± 95% CI
Dispersal - Resistance	Core	No	+0.155 (-0.246; +0.515)
Dispersal - Resistance	Core	Yes	-0.091 (-0.459; +0.299)
Dispersal - Resistance	Front	No	-0.387 (-0.761; +0.168)
Dispersal - Resistance	Front	Yes	-0.440 (-0.648; - 0.183)
r_0 - $\bar{N}$	Core	No	+0.264 (-0.336; +0.725)
r_0 - $\bar{N}$	Core	Yes	-0.459 (-0.774; -0.021)
r_0 - $\bar{N}$	Front	No	+0.080 (-0.519; 0.643)
r_0 - $\bar{N}$	Front	Yes	-0.702 (-0.888; -0.399)
Speed - Tortuosity	Core	No	-0.915 (-0.978; -0.680)
Speed - Tortuosity	Core	Yes	-0.409 (-0.738; +0.067)
Speed - Tortuosity	Front	No	-0.319 (-0.777; +0.315)
Speed - Tortuosity	Front	Yes	-0.841 (-0.944; -0.652)
Dispersal - Tortuosity	Core	No	+0.043 (-0.419; +0.506)
Dispersal - Tortuosity	Core	Yes	+0.246 (-0.210; +0.636)
Dispersal - Tortuosity	Front	No	+0.302 (-0.253; +0.726)
Dispersal - Tortuosity	Front	Yes	+0.206 (-0.119; +0.489)
Dispersal - Speed	Core	No	+0.206 (-0.119; +0.489)
Dispersal - Speed	Core	Yes	-0.136 (-0.569; +0.329)
Dispersal - Speed	Front	No	-0.249 (-0.691; +0.319)
Dispersal - Speed	Front	Yes	-0.248 (-0.528; +0.067)
Resistance- r_0	Core	No	+0.363 (-0.087; +0.694)
Resistance- r_0	Core	Yes	+0.330 (-0.057; +0.635)
Resistance- r_0	Front	No	-0.307 (-0.763; +0.297)
Resistance- r_0	Front	Yes	-0.135 (-0.441; +0.200)

786

787